Eur. Phys. J. C 53, 599–606 (2008)
DOI 10.1140/epjc/s10052-007-0489-y

THE EUROPEAN PHYSICAL JOURNAL C

Regular Article – Theoretical Physics

Neutrino hierarchy from CP-blind observables with high density magnetized detectors

A. Donini[1], E. Fernandez-Martinez[1], P. Migliozzi[2], S. Rigolin[1], L. Scotto Lavina[2,3], M. Selvi[4], T. Tabarelli de Fatis[5], F. Terranova[6,a]

[1] I.F.T. and Dep. Física Teórica, Universidad Autónoma de Madrid, Cantoblanco, 28049, Madrid, Spain
[2] I.N.F.N. Sezione di Napoli, Complesso Universitario di Monte Sant'Angelo, via Cintia, 80126, Napoli, Italy
[3] Dip. di Fisica, Università "Federico II", Complesso Universitario di Monte Sant'Angelo, via Cintia, 80126, Napoli, Italy
[4] I.N.F.N., Sezione di Bologna, Via Irnerio 46, 40129, Bologna, Italy
[5] Università di Milano Bicocca and I.N.F.N., Piazza delle Scienze 3, 20126, Milano, Italy
[6] I.N.F.N. Laboratori Nazionali di Frascati, Via E. Fermi 40, 00044, Frascati (Rome), Italy

Received: 11 June 2007 / Revised version: 31 October 2007 /
Published online: 22 December 2007 –

Abstract. High density magnetized detectors are well suited to exploit the outstanding purity and intensities of novel neutrino sources like neutrino factories and beta beams. They can also provide independent measurements of leptonic mixing parameters through the observation of atmospheric muon-neutrinos. In this paper, we discuss the combination of these observables from a multi-kT iron detector and a high energy beta beam; in particular, we demonstrate that even with moderate detector granularities the neutrino mass hierarchy can be determined for θ_{13} values greater than 4°.

PACS. 14.60.Pq; 14.60.Lm

1 Introduction

In the standard interpretation of the experimental evidence for neutrino oscillations [1–10], the squared-mass differences among the ν mass eigenstates (m_1, m_2 and m_3) are rather hierarchical: $\Delta m^2_{21} \equiv m^2_2 - m^2_1 \simeq 1/30 \times |\Delta m^2_{32}| \simeq |\Delta m^2_{31}|$. The small size of Δm^2_{21} is implied by solar and long-baseline reactor neutrino data. In this framework, particularly enlightening are the oscillations at the "atmospheric scale", i.e. when $|\Delta m^2_{32}|L/4E \simeq \pi/2$, L and E being the neutrino energy and path-length, respectively. A muon-neutrino oscillating at the atmospheric scale undergoes mainly $\nu_\mu \to \nu_\tau$ transitions. This dominant mode is implied by long-baseline accelerator experiments, atmospherics and short-baseline reactor data; moreover, it is currently under test in a direct manner at CNGS [11]. We have no evidence of subdominant $\nu_\mu \to \nu_e$ transitions at such scale, implying a small mixing angle between the first and third mass eigenstate ($\theta_{13} < 10^\circ$ at 90% C.L. [12–14]). If θ_{13} is non-zero, the subdominant $\nu_\mu \to \nu_e$ amplitude and its T or CP conjugates encode a wealth of information. In particular, it allows for the determination of θ_{13} and the Dirac complex phase of the leptonic mixing matrix. The $\nu_\mu \to \nu_e$ transition probability is also perturbed by matter effects if the path of the neutrinos through the earth is sufficiently large. The perturbation depends on the sign of Δm^2_{31} and therefore it allows for the determination of the hierarchy among the neutrino masses. These considerations explain the enormous interest in novel neutrino sources operating at the atmospheric scale [15] like, for instance, neutrino factories [16–18] or beta beams [19]. Combination of these facilities with more traditional measurements of atmospheric neutrinos has also been considered [20–24]. Such a combination is particularly natural when the detector at the far location is dense and capable of charge reconstruction: this is the case for magnetized iron calorimeters, which can perform detailed measurements of atmospheric ν_μ fluxes and are recognized as ideally suited to exploit a possible neutrino factory or high energy beta beam [25–33]. However, it is generally believed that the contribution of atmospheric neutrinos is marginal for any realistic configuration, unless the value of the θ_{13} angle turns out to be very close to current bounds [34]. In this paper, we carry out a more detailed analysis of the atmospheric data that can be collected by a 40-kT magnetized iron calorimeter (Sect. 3). This analysis is tuned so as to be able to identify the occurrence of resonant transitions in the earth, and it is combined with the data that can be collected by the same detector exposed to a high energy beta beam [27] at a baseline of ~ 700 km (Sect. 4). The sensitivity of the atmospheric data to the neutrino mass hierarchy does not depend on the value of δ ("CP-blind") but it is highly deteriorated by the lack

[a] e-mail: francesco.terranova@cern.ch

of knowledge of θ_{13}; on the other hand, the beta beam data exhibit a very strong dependence on δ but provide tight constraints on the size of the θ_{13}. Their combination (Sect. 5) results in a significantly improved capability to determine the hierarchy of the neutrino mass eigenstates.

2 Atmospheric and long-baseline oscillations

Current experimental data are unable to fix uniquely the hierarchy of neutrino masses [1], i.e. whether the m_1 eigenstate is lighter than m_3 ($m_1 < m_2 < m_3$: "normal hierarchy") or heavier ($m_3 < m_1 < m_2$: "inverted hierarchy"). Clearly, this pattern is of great theoretical relevance because it allows for discrimination among models that explain neutrino masses [35]. In vacuum, observables sensitive to the mass pattern exist but their exploitation is extremely challenging from the experimental point of view [36–39]. However, propagation in matter can enhance the perturbations to the transition probabilities due to the sign of Δm^2_{31} and, for sizable values of θ_{13} such perturbations become observable even with present technologies. In particular, the $\nu_e \to \nu_\mu$ transition amplitude (or its T and CP conjugate) encodes an explicit dependence on the sign of Δm^2_{31} [40–42]:

$$
\begin{aligned}
P_{\nu_e\to\nu_\mu} \simeq\ & \sin^2 2\theta_{13} \sin^2\theta_{23} \frac{\sin^2[(1-\hat{A})\Delta]}{(1-\hat{A})^2} \\
& + \alpha \sin 2\theta_{13}\xi \sin\delta \sin(\Delta) \frac{\sin(\hat{A}\Delta)}{\hat{A}} \frac{\sin[(1-\hat{A})\Delta]}{(1-\hat{A})} \\
& + \alpha \sin 2\theta_{13}\xi \cos\delta \cos(\Delta) \frac{\sin(\hat{A}\Delta)}{\hat{A}} \frac{\sin[(1-\hat{A})\Delta]}{(1-\hat{A})} \\
& + \alpha^2 \cos^2\theta_{23} \sin^2 2\theta_{12} \frac{\sin^2(\hat{A}\Delta)}{\hat{A}^2} \,. \qquad (1)
\end{aligned}
$$

In this formula $\Delta \equiv \Delta m^2_{31} L/(4E)$ and the terms contributing to the Jarlskog invariant are split into the small parameter $\sin 2\theta_{13}$, the $\mathcal{O}(1)$ term $\xi \equiv \cos\theta_{13} \sin 2\theta_{12} \sin 2\theta_{23}$ and the CP term $\sin\delta$; $\hat{A} \equiv 2\sqrt{2} G_{\rm F} n_e E/\Delta m^2_{31}$ with $G_{\rm F}$ the Fermi coupling constant and n_e the electron density in matter. Note that the sign of $\hat{A}$ depends on the sign of Δm^2_{31} which is positive (negative) for normal (inverted) hierarchy of neutrino masses.

For a monochromatic beam, a $\nu_e \to \nu_\mu$ run combined with its CP conjugate $\bar{\nu}_e \to \bar{\nu}_\mu$ cannot determine uniquely sign(Δm^2_{31}) for all values of δ. In particular, if the hierarchy is normal (inverted) and $\delta < 0$ ($\delta > 0$), it is always possible to find a solution that reproduces the correct $\nu_e \to \nu_\mu$ and $\bar{\nu}_e \to \bar{\nu}_\mu$ rate assuming the wrong hypothesis on sign(Δm^2_{31}). For beams of finite width, spectral information help lifting this ambiguity, but, in general, they require very large statistics and excellent detector resolution. Figures 1 and 2 show the allowed θ_{13}, δ region from a neutrino and antineutrino run of a Super-SPS [43, 44] based beta beam assuming both the wrong (red) and right (green) hypothesis.[1] The true parameters are $\theta_{13} = 4°$, sign(Δm^2_{31}) $= +1$ and $\delta = 90°$ (Fig. 1) or $\delta = -90°$ (Fig. 2). The existence of overlapping regions in Fig. 2 testifies to the consistency of the wrong hypothesis with the accelerator data. In general, we expect a highly deteriorated sensitivity to mass hierarchy for nearly 50% of the possible true values of δ. This is clearly visible in Fig. 8 of [27] and it is reproduced in Fig. 6 (blue line).[2]

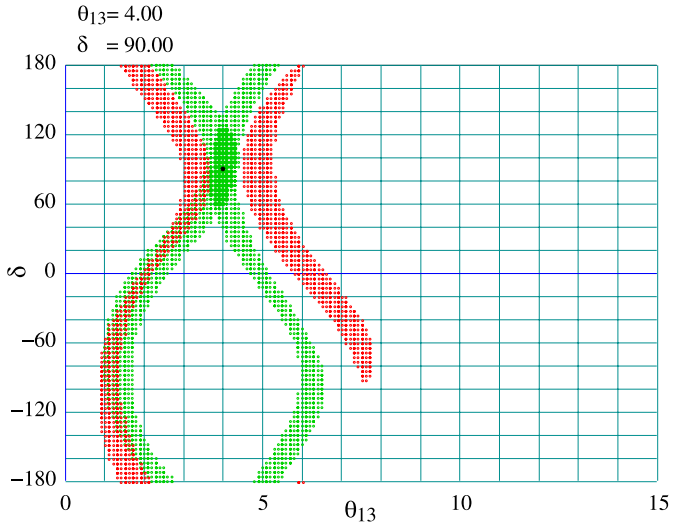

Fig. 1. Allowed θ_{13}, δ regions from a neutrino and antineutrino run of a Super-SPS based beta beam assuming the wrong (*inverted, red*) and right (*normal, green*) mass hierarchy hypothesis. The true parameters are $\theta_{13} = 4°$, sign(Δm^2_{31}) $= +1$ and $\delta = 90°$

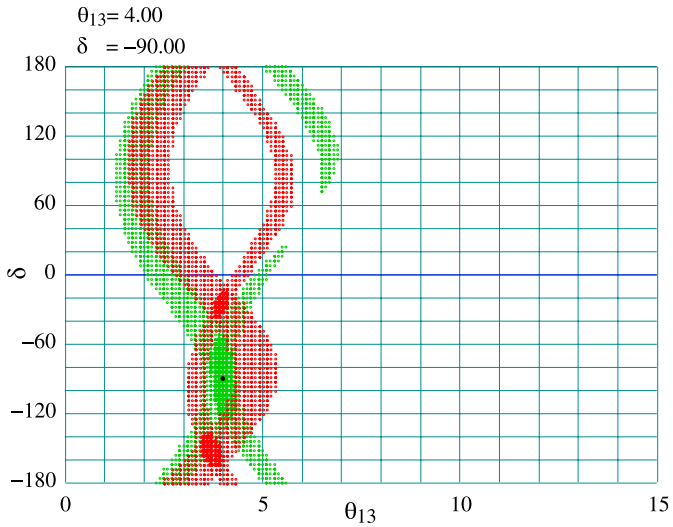

Fig. 2. As in Fig. 1 with $\delta = -90°$. Overlapping regions are present also for the wrong hypothesis (*red area*)

[1] Details on this experimental setup are given in [27] and are briefly recalled in Sect. 3.

[2] Actually, most of the next generation long-baseline experiments proposed so far suffer from this limitation. For an example based on superbeams we refer to [45].

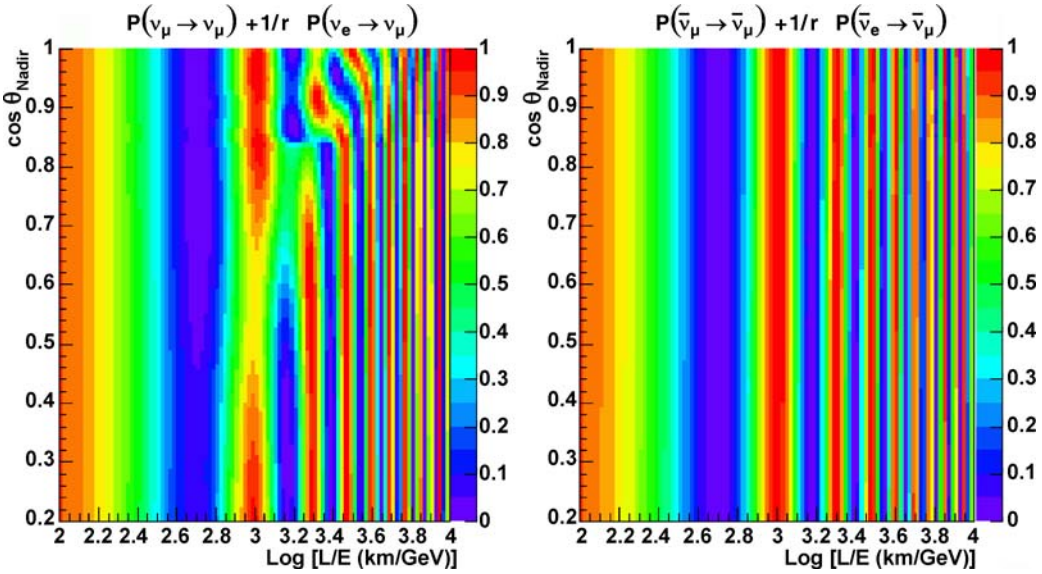

Fig. 3. Probability of observing atmospheric muon neutrinos (*left plot*; antineutrinos are shown in the *right plot*) from $\nu_\mu \to \nu_\mu$ and $\nu_e \to \nu_\mu$ transitions as a function of L/E and the Nadir angle θ ($\sin^2 2\theta_{13} = 0.1$, $\Delta m^2_{31} = 2.5 \times 10^{-3}$ eV^2). In the *upper label*, r is the ratio between the initial ν_μ and ν_e fluxes

Since the dependence on δ and, in general, the three-family interference effects are the origin of this ambiguity, a substantial improvement can be achieved exploiting CP-blind observables. In $\nu_e \to \nu_\mu$ transitions, CP-blindness can be achieved introducing a phase advance (increase of baseline) such that the phase acquired by neutrinos due to interaction with matter equals 2π [46, 47]. It can be shown [48] that this condition is equivalent to choosing $L = 2\pi/\sqrt{2}G_{\rm F}n_e$, i.e. finding a L such that the last three terms of (1) cancel. Such a baseline is dubbed "magic" in the literature [46, 47], and it is proportional to the energy and width of the MSW resonance in a medium of constant density:

$$E_{\rm R} = \pm\Delta m^2_{31} L_{\rm magic} \cos 2\theta_{13}/4\pi\,, \qquad (2)$$

$$\Gamma_{\rm R} = |\Delta m^2_{31}| L_{\rm magic} \sin 2\theta_{13}/2\pi\,, \qquad (3)$$

the + (−) sign referring to neutrinos (antineutrinos). A similar approach can be pursued using atmospheric neutrinos. In this case, however, additional difficulties are present. First of all, the initial flux is a mixture of ν_μ, ν_e and their antiparticles. Moreover, the approximation of constant density is not tenable and core-mantle interference effects are possible. Finally, the detector resolution must be sufficient to identify the region where the MSW resonance occurs. In turn, the latter condition is a requirement on the size of θ_{13} through (3). Equation (2) implies that the resonance condition can occur only for neutrinos if the hierarchy is normal and only for antineutrinos if the hierarchy is inverted. Hence, the task of fixing the hierarchy is reduced to the issue of determining the occurrence of this resonance or at least the spectral perturbation induced by it in the neutrino (antineutrino) sample. Such a perturbation is depicted in Fig. 3 for $\sin^2 2\theta_{13} = 0.1$ (normal hierarchy) as a function of L/E and the Nadir angle θ of the neutrinos. It has been computed solving numerically [49] the Schroedinger equation for the propagation of neutrinos in matter and assuming the earth density profile of [50]. For all currently allowed values of $\Delta m^2_{21}/|\Delta m^2_{32}|$, three-family interference effects are negligible in the multi-GeV neutrino sample [34] ($E > 1.5$ GeV) and, therefore, the observables are completely CP-blind.

3 Experimental setup

The experimental setup considered in this paper closely follows the configuration studied in [27]. It exploits a possible novel source operating in $\nu_e \to \nu_\mu$ mode, i.e. a beta beam leveraging an upgraded injection complex for the LHC. The beta beams are pure sources of electron-neutrinos obtained producing, accelerating and stacking beta-unstable isotopes. The most advanced machine study regarding this novel approach is currently in progress within the Eurisol Design Study group [51]; it is based on existing CERN accelerating machines (PS and SPS) and uses ^{6}He and ^{18}Ne as $\bar\nu_e$ and ν_e emitters, respectively.

Compared with such a baseline configuration, the setup of [27], which was originally proposed in [25, 26] for a massive water Cherenkov detector, considers a higher energy proton injector to the LHC (the "Super-SPS" instead of the existing SPS) employed to increase the γ of the ions; in this case, the neutrinos have energies exceeding 1 GeV. The corresponding spectra are recalled in Fig. 4. They are computed assuming the far detector to be located 730 km from CERN (CERN to Gran Sasso distance) and the ions accelerated up the same γ ($\gamma = 350$) both for ^{6}He and for ^{18}Ne ("$\gamma = 350, 350$ option"[3]) or up to the maximum rigid-

[3] ^{6}He and ^{18}Ne having nearly the same Q value, equal γ corresponds to equal average neutrino energy.

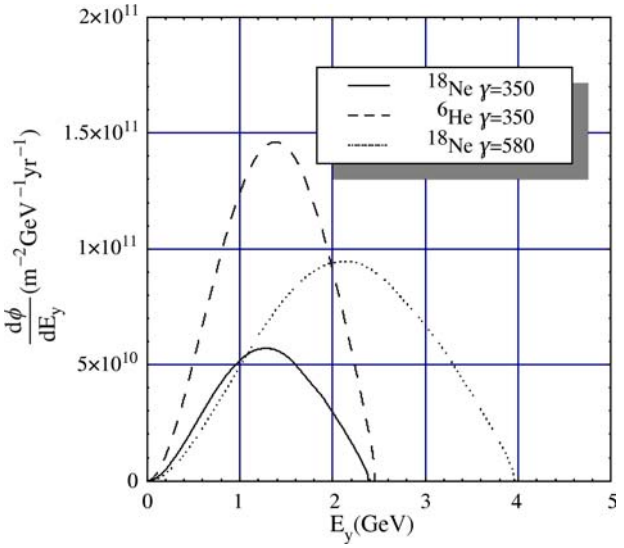

Fig. 4. Neutrino spectra at the far location

ity allowed by the Super-SPS ($\gamma = 580$ for ^{18}Ne, $\gamma = 350$ for ^{6}He). At these energies, final state muons produced by ν_μ charged-current interactions have a range significantly larger than the pion interaction length in iron. Hence, muon identification against the bulk of ν_e CC and NC interactions becomes possible even for high density iron detectors. Differently from the case of the Neutrino Factories, the far detector does not require charge identification capability: the initial state ν_e beam is free from $\bar{\nu}_\mu$ contaminations and μ^+ production from charm or tau decays is kinematically suppressed. In this context, the only advantage of magnetization comes from the additional suppression of the NC background with a pion misidentified as a muon.

In [27], the detector was based on glass resistive plate chambers interleaved with 4 cm thick vertical iron slabs. The fiducial mass is 40 kT i.e. the detector can be accommodated in one of the existing LNGS experimental halls. The RPC are housed in a 2 cm gap and the signal is read out on external pick-up electrodes segmented in $2 \times 2\,\mathrm{cm}^2$ pads. This detector can be divided into large modules (about 15 m length) and magnetized by copper coils running through the slabs. This design, which resembles the toroidal configuration of MINOS, was studied in detail by the MONOLITH Collaboration in 1999 [52] and it has been recently revived by the Indian proposal INO [53, 54]. Hence, the far detector of [27] represents a unique atmospheric neutrino detector. In particular, MONOLITH studies[4] have demonstrated that the vertical orientation of the steel does not compromise the capability of reconstructing the oscillation pattern of atmospheric neutrinos. Moreover, the atmospheric analysis profits of the higher granularity needed for the accelerator-based ν_μ appearance search.

[4] The interest for a vertical slab configuration was originally motivated by the possible exploitation of MONOLITH at CNGS (see [52] Chapter 2).

In the following, we consider a 40 kT magnetized detector running at a beta beam for 10 years. The accelerator facility is assumed to provide 2.9×10^{18} ^{6}He and 1.1×10^{18} ^{18}Ne decays per year. As in [27], we stress that no solid estimates of fluxes are available for the Super-SPS option: we refer to [27] for a systematic study of the sensitivity as a function of fluxes.

4 Analysis of atmospheric data

The simulation of atmospheric events at the far detector for the beta beam is similar to the one recently implemented by MINOS [55]: flux expectations are based on the Bartol 96 [56] model and interactions have been calculated with GRV94 [57] parton distributions including contributions from quasi-elastic and single pion production [49]. The detector response has been fully simulated with GEANT3 [58] assuming the magnetic field maps resulting from the coil arrangement of MONOLITH. The average magnetic field along the slabs is ~ 1.3 T.

As discussed in Sect. 2, a substantial enhancement of the sensitivity to hierarchy can be obtained tuning the event selection so as to be able to identify the region where resonant enhancement occurs. The resonance appears as a perturbation to the original L/E pattern for a given earth matter density. For $\cos\theta > 0.85$ the neutrinos cross the earth core and resonant conversions can appear already at a few GeV ($E_\mathrm{R} \simeq 3$ GeV). At smaller $\cos\theta$, the ν intersect the earth mantle and crust, and resonances appear at larger E_R (~ 7 and ~ 11 GeV respectively). Hence, a two dimensional analysis either in E versus L or, equivalently, in L/E versus $\cos\theta$ is appropriate to extract information on the existence and location of earth matter resonances. The choice of the L/E variable allows for the implementation of the Monolith criteria for the observability of the sinusoidal pattern [52] to the search for resonant conversion. This approach has been developed in [49], where the expected resolution on L and E is computed on an event-by-event basis; here, events are retained only if the expected resolution is adequate (FWHM on L/E smaller than 50%) in the region of interest for matter effect perturbations. A preselection is applied requiring a minimum muon energy of 1.5 GeV; only internal events are considered: they can be either fully contained or with a single outgoing track ranging out of the detector with a visible path-length greater than 4 m. On average, these requirements result in a selection efficiency that is negligible below 3 GeV and nearly constant ($\sim 55\%$) above 5 GeV. At these energies, charge misidentification is well below 5% and therefore, rather pure μ^+ and μ^- samples can be collected.

Figure 5 (left) shows the L/E distribution of selected events corresponding to 400 kT year (10 years of data taking) for $\Delta m^2_{31} = 2.5 \times 10^{-3}\,\mathrm{eV}^2$, $\sin^2 2\theta_{13} = 0.1$ and $\theta_{23} = 45°$. In this figure, also down-going events are shown: they are used as an unoscillated reference sample to reduce the systematics due to the uncertainty on the initial fluxes. The ratio up-going/down-going is shown in Fig. 5

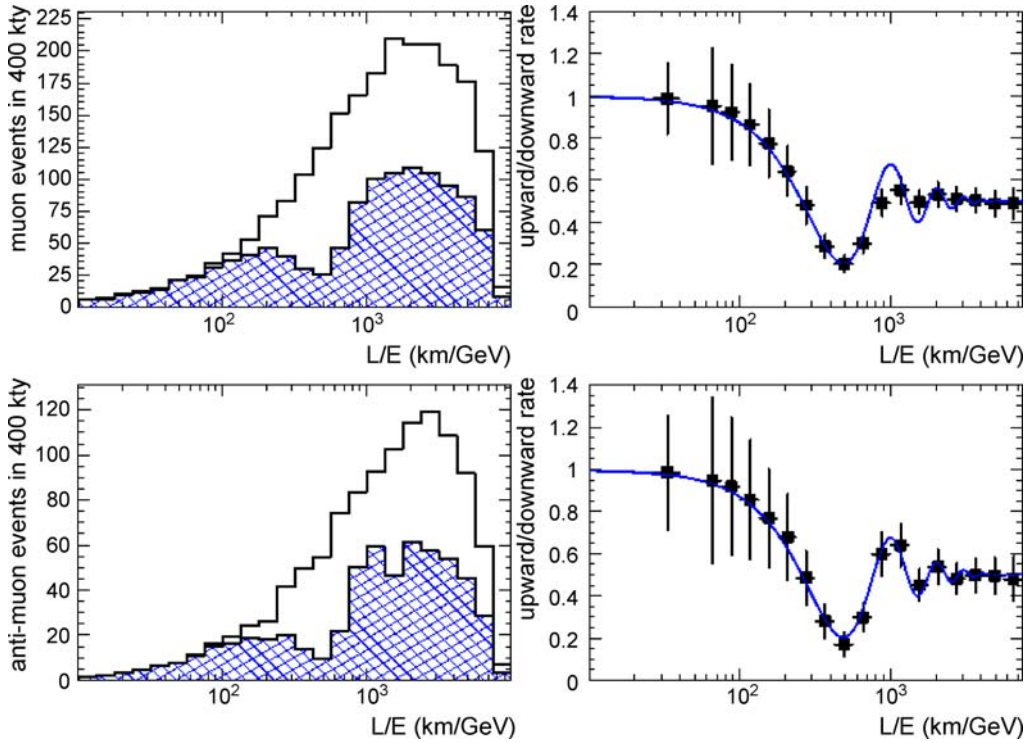

Fig. 5. L/E distribution of selected events corresponding to 400 kT yr (10 year of data taking) for $\Delta m^2_{31} = 2.5 \times 10^{-3}$ eV^2, $\sin^2 2\theta_{13} = 0.1$ and $\theta_{23} = 45^\circ$ (*left upper*: neutrinos, *left lower*: antineutrinos). The *shaded (unshaded) histogram* corresponds to the sample of up-going (down-going) neutrinos. For illustration of the effect, the ratio up-going/down-going is also shown (*right*) together with a fit that assumes $\theta_{13} = 0^\circ$

(right); the fit assumes $\theta_{13} = 0^\circ$: perturbations due to matter effects and finite θ_{13} are visible only for neutrinos since normal hierarchy is assumed; moreover, distortions with respect to pure $\nu_\mu \to \nu_\tau$ oscillations are present mainly beyond the first minimum of the survival probability.

5 Sensitivity to mass hierarchy

The determination of mass hierarchy from atmospheric neutrinos is plagued by the uncertainty on the mixing parameters, particularly on θ_{13}. Accelerator neutrino experiments (a beta beam in the present case) can provide very strong constraints on this angle, once marginalized over δ. In particular, the manifold of the allowed θ_{13}, δ values is highly reduced by running both in $\nu_e \to \nu_\mu$ and in its CP conjugate mode (antineutrino run). Hence the combination of accelerator and atmospheric data can be rather effective [23, 24].

5.1 Likelihood analysis

The analysis of accelerator data employed in the following does not differ from the one described in [27]: we refer to that reference for the details of event selection and detector performance. The sensitivity to the sign of Δm^2_{31} is computed from a likelihood analysis that combines the allowed θ_{13} range resulting from the beta beam run with the atmospheric likelihood:

$$\ln \mathcal{L} = \ln \prod_{i,q} \left[\frac{\mathrm{e}^{-A_q \mu_{i,q}} (A_q \mu_{i,q})^{U_{i,q}}}{U_{i,q}!} \right] - \sum_q \frac{1}{2} \frac{(A_q - 1)^2}{\sigma_A^2} , \tag{4}$$

where the subscripts i and q are referred to bins in the $(\cos\theta,\ L/E)$ plane and of muon charge respectively; $U_{i,q}$ and $A_q \mu_{i,q}$ are the observed and expected number of up-going neutrino events in the i, q bin and the last term in the likelihood accounts for the overall normalization uncertainty for neutrinos and antineutrinos separately: further details on the treatment of systematics and their relevance for the mass hierarchy determination are provided below (Sect. 5.2). Additional penalty terms of the form $(P - P_{\mathrm{best}})^2/2\sigma^2$ are added to (4) to account for the uncertainty on $P = |\Delta m^2_{31}|$ and $P = \theta_{23}$. Here, P_{best} is the current best estimate of the parameter and σ the estimated precision. The latter is the current precision for θ_{23} and the expected one at the end of T2K for $|\Delta m^2_{31}|$. For each "true" value of θ_{13}, δ and the sign of Δm^2_{31} (e.g. +1 for normal hierarchy), we compute the C.L. of the best fit for the wrong hypothesis (e.g. $\mathrm{sign}(\Delta m^2_{31}) = -1$). Figure 6 shows the region where the wrong hypothesis is excluded at 90, 95 and 99% C.L. This figure demonstrates what has been stated qualitatively in Sect. 2: due to the insensitivity to the Dirac phase, the cancellation effect

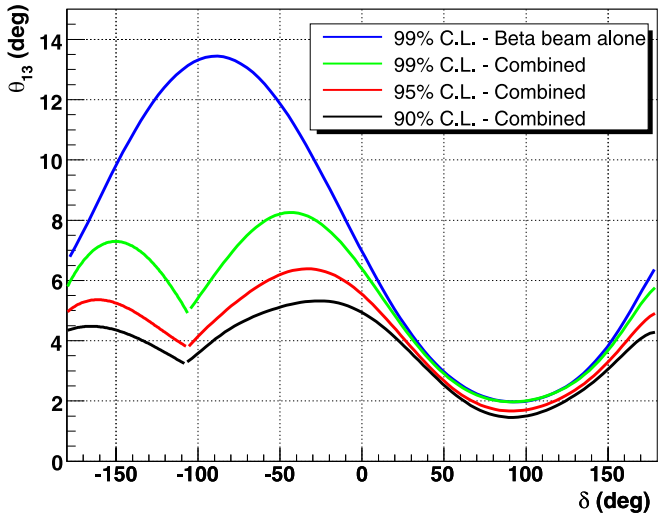

Fig. 6. Region of the true value of the parameters θ_{13} and δ where the correct neutrino hierarchy (assumed to be normal in this figure) can be distinguished from the wrong one at 90, 95 and 99% C.L. Data from the beta beam only are also shown

that equals the rates of μ^+ and μ^- at the beta beam does not take place with atmospherics. Hence, atmospheric data are relevant and, actually, dominate the sensitivity to mass hierarchy in most of the beta beam blind region. In the present scenario, hierarchy can be determined at 90% C.L. down to $\theta_{13} \simeq 4°$. At positive (negative) δ and normal (inverted) hierarchy, the beta beam data dominates and sign(Δm^2_{31}) can be extracted down to $\theta_{13} \simeq 2°$. Compared with stand-alone analysis of atmospheric neutrinos with high density detectors [49], where some sensitivity can be achieved only for θ_{13} values very close to current CHOOZ limits, here the accelerator-based determination of this parameter pushes the sensitivity to the mass hierarchy down to $\sin^2 2\theta_{13} \simeq 0.02$ even for very unfavorable values of the Dirac phase δ. This is illustrated in Fig. 7 where the likelihoods for the atmospheric sample only are shown for $\theta_{13} = 5°$. The left (right) plots assume normal (inverted) hierarchy as the true hierarchy. In general, Fig. 7 shows that hierarchy separation cannot be achieved if θ_{13} is completely unconstrained: on the other hand, even for the most unfavorable values of δ, the beta beam provides stringent limits to θ_{13} that makes the atmospheric sample a sensitive tool for hierarchy determination. If the true hierarchy is inverted, distortions will appear in the antineutrino sample, i.e. in the atmospheric sample with lower statistics due to the difference between ν_μ and $\bar{\nu}_\mu$ cross sections. However, the discrimination power depends on the difference between the higher statistics ν_μ sample and the lower statistics $\bar{\nu}_\mu$ one and, as visible from Fig. 7, the power of the test is practically the same both assuming normal and inverted "true" hierarchy.

The use of the Monolith criteria for event selection improves substantially the sensitivity with respect to analyses in which flat resolutions have been assumed [34]. In spite of their limited mass, high density atmospheric detectors compete with megaton-size water Cherenkov ones thanks to the capability of measuring the sign of the multi-GeV sample. On the other hand, due to larger statistics, accelerator data are sensitive to perturbations induced by the sign of Δm^2 up to $\sin^2 2\theta_{13} \simeq 0.03$–$0.02$ (see Fig. 16 of [24]). Finally, it is worth noting that significantly better results (sensitivities to the hierarchy down to $\sin^2 2\theta_{13} < 0.01$) could be achieved by dedicated detectors located at the magic baseline without the use of atmospheric sample [30, 31]. These setups, however, require either large boosters for the beta beam ions (LHC) or novel ions with larger Q values and increased flux to compensate for the losses at the far location [32, 33]. Moreover, no information on CP violation in the leptonic sector would be accessible and a second detector at a closer distance from the source would be needed.

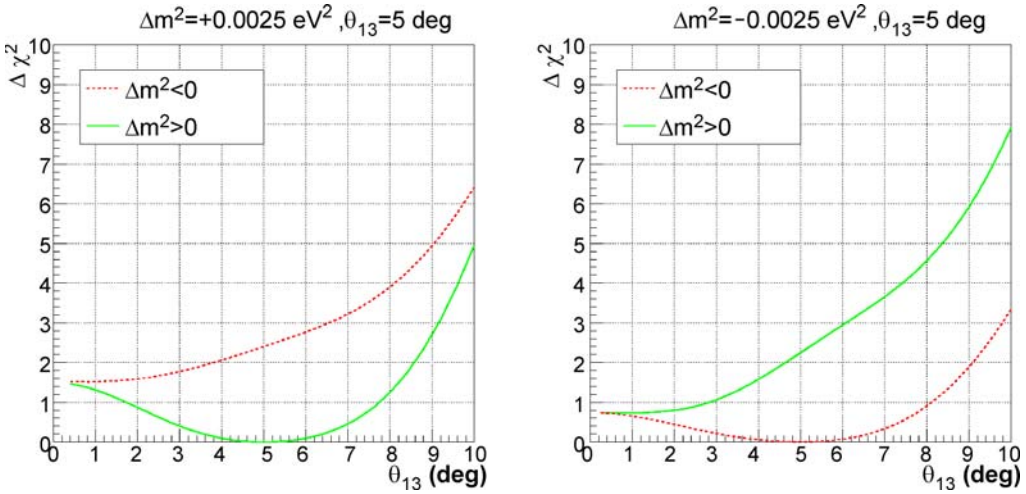

Fig. 7. Likelihoods of the atmospheric sample ($\Delta\chi^2 \equiv -2\log(L/L_{\max})$) as a function of θ_{13} assuming a normal hierarchy (*left plot*) or inverted hierarchy (*right plot*) as true hierarchy and $\theta_{13} = 5°$. The *continuous green line* is the likelihood for $\Delta m^2 > 0$ (right hypothesis in the *left plot*, wrong hypothesis in the *right plot*) and the *dashed red line* is for $\Delta m^2 < 0$

5.2 Systematic uncertainties for the atmospheric sample

Systematic uncertainties on the rate of multi-GeV and sub-GeV samples of atmospheric neutrinos have been studied in depth in the literature due to their relevance for the determination of the leading oscillation parameters Δm_{13} and $\sin^2\theta_{23}$. Moreover, they affect the pattern of muon disappearance and the perturbation of the ν_e sample and, therefore, they can be limiting factors in the determination of the mass hierarchy and θ_{13}. In our case, the knowledge of θ_{13} is completely dominated by accelerator data, while the determination of the mass hierarchy is mainly related to the location of the MSW resonance in the neutrino or antineutrino sample. Hence, several systematic contributions that currently limit the knowledge of the leading parameters at atmospheric detectors (overall flux and cross section normalization, ν_μ/ν_e ratio, zenith and energy dependence of the differential fluxes) play here a minor role. In order to probe quantitatively such a statement, in the present analysis systematic uncertainties have been treated following the approach developed by the Monolith collaboration and based on up–down differential normalization [52, 59]. For each bin in the L/E distribution of the up-going neutrinos, the unoscillated sample is taken from the corresponding down-going one. Here "up-going" means that neutrinos reach the detector coming from below the horizon ($\cos\theta > 0$); the "corresponding down-going" ones are neutrinos whose Nadir angle θ' is such that $\theta' = \pi - \theta$. This subsample provides a nearly theory-free normalization, since the uncertainties on the flux and cross sections affecting the population of such bin cancel out because of the spherical symmetry and the isotropy of the primary cosmic ray flux. Further details and interesting subtleties can be found in the Monolith proposal [52]. For instance, geomagnetic effects can introduce an asymmetry in the up/down sample that could be interpreted as a perturbation of the L/E pattern. However, for the multi-GeV sample selected in this analysis, with a minimum neutrino energy of 3 GeV (see Sect. 4), this effect is negligible [60]. Yet, an overall penalty term in the flux normalization has been introduced (see (4)), to cope with the ν_μ/ν_e ratio uncertainty, as the proposed detector cannot directly measure the ν_e flux. This approach is somewhat conservative: in most of the cases, the present theoretical knowledge of the atmospheric fluxes exceeds the statistical precision of the down-going samples for bin widths comparable to the detector resolution. However, for the present case, in which systematics plays a less important role than for the leading parameter analysis, this technique simplifies remarkably the treatment of systematics without compromising the sensitivity to the mass hierarchy. To ease comparison with other analyses (see e.g. Table 1 of [34]) we note that the statistical uncertainty of the down-going sample in the region where the oscillation dip at θ_{13} is located is about 9%, while typical differential uncertainties in the rate of multi-GeV ν_μ are of the order of 5%. Moreover, the down-going normalization sample is measured for neutrinos and antineutrinos separately, hence assuming that the uncertainty on the $\nu_\mu/\bar{\nu}_\mu$ ratio could also have a dependence in energy and in direction, while in most of the analyses a flat uncertainty of about 5% is considered. As a consistency check, we artificially decreased the statistical uncertainty of the down-going sample up to 3% noting that the sensitivity to the sign of Δm^2_{31} remains practically unchanged. This is in agreement to what already had been observed by some authors, i.e. that "the discrimination between normal and inverted hierarchy is based on a very characteristic signal consisting of pronounced structures in the E and $\cos\theta$ distributions, which cannot easily be mimicked by the systematic effects" [34].

The most relevant systematic uncertainty of instrumental origin is related to the pollution of the neutrino sample with antineutrinos due to charge misassignment. In most of the analyses presented in the literature, an overall uncertainty in knowledge of the charge (typically 5%) is assumed independently of the topology of event. The present analysis, instead, is based on a full GEANT3 simulation of the detector, followed by a reconstruction stage with track fitting. Neutrino flavor assignment is based on the reconstructed muon charge, thus encompassing a realistic energy and event shape dependency, as far as GEANT3 can predict the behavior of magnetised iron calorimeters.[5] The charge misidentification systematics is the most relevant detector-dependent systematics in the atmospheric analysis, while it is immaterial in the beta beam analysis, where π/μ misidentification dominates. This is the reason why we assumed the systematics of the accelerator and atmospheric data to be fully uncorrelated.

6 Conclusions

Detailed atmospheric neutrino studies can be done in several detectors that have been built or proposed for long-baseline accelerator facilities. In particular, high density magnetized detectors can study multi-GeV atmospheric neutrinos and distinguish between ν_μ and $\bar{\nu}_\mu$. These data can be combined in a highly non-trivial manner to improve the sensitivity to the neutrino mass hierarchy. In this paper we considered in particular a high energy beta beam with a 40 kT iron calorimeter located at the CERN to Gran Sasso distance. The atmospheric data collected by this detector allows for the determination of the neutrino hierarchy down to $\theta_{13} \simeq 4^\circ$ in the region of δ where the corresponding beta beam data cannot constrain the sign of Δm^2_{31}. Far from this blind region, the beta beam data dominates and sign(Δm^2_{31}) can be extracted down to $\theta_{13} \simeq 2^\circ$ at 90% C.L.

Acknowledgements. We wish to express our gratitude to S. Petcov, S. Agarwalla and A. Blondel for several useful discussions during the WIN07 workshop in Kolkata.

[5] Solid testbeds are based, e.g., on the CDHS and MINOS data, on non-compensated hadronic calorimeters at colliders and on Monolith testbeams [61].

References

1. Particle Data Group, W.M. Yao et al., J. Phys. G **33**, 1 (2006) and references therein
2. SNO Collaboration, Q.R. Ahmad et al., Phys. Rev. Lett. **87**, 071 301 (2001)
3. SNO Collaboration, B. Aharmim et al., Phys. Rev. C **72**, 055 502 (2005)
4. KamLAND Collaboration, T. Araki et al., Phys. Rev. Lett. **94**, 081 801 (2005)
5. Super-Kamiokande Collaboration, Y. Ashie et al., Phys. Rev. D **71**, 112 005 (2005)
6. MACRO Collaboration, M. Ambrosio et al., Phys. Lett. B **566**, 35 (2003)
7. K2K Collaboration, E. Aliu et al., Phys. Rev. Lett. **94**, 081 802 (2005)
8. Super-Kamiokande Collaboration, K. Abe et al., Phys. Rev. Lett. **97**, 171 801 (2006)
9. Super-Kamiokande Collaboration, J. Hosaka et al., Phys. Rev. D **74**, 032 002 (2006)
10. MINOS Collaboration, D.G. Michael et al., Phys. Rev. Lett. **97**, 191 801 (2006)
11. OPERA Collaboration, R. Acquafredda et al., New J. Phys. **8**, 303 (2006)
12. CHOOZ Collaboration, M. Apollonio et al., Eur. Phys. J. C **27**, 331 (2003)
13. CHOOZ Collaboration, M. Apollonio et al., Phys. Lett. B **466**, 415 (1999)
14. Palo Verde Collaboration, F. Boehm et al., Phys. Rev. D **64**, 112 001 (2001)
15. A. Guglielmi, M. Mezzetto, P. Migliozzi, F. Terranova, arXiv:hep-ph/0508034 (in D. Bettoni et al., Phys. Rep. **434**, 47 (2006), pp. 68–87)
16. S. Geer, Phys. Rev. D **57**, 6989 (1998)
17. S. Geer, Phys. Rev. D **59**, 039 903 (1999) [Erratum]
18. A. De Rujula, M.B. Gavela, P. Hernandez, Nucl. Phys. B **547**, 21 (1999)
19. P. Zucchelli, Phys. Lett. B **532**, 166 (2002)
20. J. Bernabeu, S. Palomares Ruiz, S.T. Petcov, Nucl. Phys. B **669**, 255 (2003)
21. M.C. Gonzalez-Garcia, M. Maltoni, Eur. Phys. J. C **26**, 417 (2003)
22. M.C. Gonzalez-Garcia, M. Maltoni, A.Y. Smirnov, Phys. Rev. D **70**, 093 005 (2004)
23. P. Huber, M. Maltoni, T. Schwetz, Phys. Rev. D **71**, 053 006 (2005).
24. J.E. Campagne, M. Maltoni, M. Mezzetto, T. Schwetz, JHEP **0704**, 003 (2007)
25. J. Burguet-Castell, D. Casper, J.J. Gomez-Cadenas, P. Hernandez, F. Sanchez, Nucl. Phys. B **695**, 217 (2004)
26. J. Burguet-Castell, D. Casper, E. Couce, J.J. Gomez-Cadenas, P. Hernandez, Nucl. Phys. B **725**, 306 (2005)
27. A. Donini, E. Fernandez-Martinez, P. Migliozzi, S. Rigolin, L. Scotto Lavina, T. Tabarelli de Fatis, F. Terranova, Eur. Phys. J. C **48**, 787 (2006)
28. P. Huber, M. Lindner, M. Rolinec, W. Winter, Phys. Rev. D **73**, 053 002 (2006)
29. F. Terranova, A. Marotta, P. Migliozzi, M. Spinetti, Eur. Phys. J. C **38**, 69 (2004)
30. S.K. Agarwalla, A. Raychaudhuri, A. Samanta, Phys. Lett. B **629**, 33 (2005)
31. S.K. Agarwalla, S. Choubey, A. Raychaudhuri, Nucl. Phys. B **771**, 1 (2007)
32. C. Rubbia, A. Ferrari, Y. Kadi, V. Vlachoudis, Nucl. Instrum. Methods A **568**, 475 (2006)
33. A. Donini, E. Fernandez-Martinez, Phys. Lett. B **641**, 432 (2006)
34. S.T. Petcov, T. Schwetz, Nucl. Phys. B **740**, 1 (2006)
35. C.H. Albright, M.C. Chen, Phys. Rev. D **74**, 113 006 (2006)
36. A. de Gouvea, J. Jenkins, B. Kayser, Phys. Rev. D **71**, 113 009 (2005)
37. H. Minakata, H. Nunokawa, S.J. Parke, R.Z. Funchal, Phys. Rev. D **74**, 053 008 (2006)
38. H. Minakata, H. Nunokawa, S.J. Parke, R.Z. Funchal, Phys. Rev. D **76**, 053 004 (2007)
39. H. Minakata, H. Nunokawa, S.J. Parke, R.Z. Funchal, Phys. Rev. D **76**, 079 901 (2007) [Erratum]
40. A. Cervera et al., Nucl. Phys. B **579**, 17 (2000)
41. A. Cervera et al., Nucl. Phys. B **593**, 731 (2001) [Erratum]
42. M. Freund, Phys. Rev. D **64**, 053 003 (2001)
43. O. Bruning et al., LHC luminosity and energy upgrade: A feasibility study, CERN-LHC-PROJECT-REPORT-626, 2002
44. W. Scandale, Nucl. Phys. Proc. Suppl. **154**, 101 (2006)
45. NOvA Collaboration, D.S. Ayres et al., arXiv:hep-ex/0503053
46. V. Barger, D. Marfatia, K. Whisnant, Phys. Rev. D **65**, 073 023 (2002)
47. P. Huber, W. Winter, Phys. Rev. D **68**, 037 301 (2003)
48. A.Y. Smirnov, arXiv:hep-ph/0610198
49. T. Tabarelli de Fatis, Eur. Phys. J. C **24**, 43 (2002)
50. A.M. Dziewonski, D.L. Anderson, Phys. Earth Planet. Int. **25**, 297 (1981)
51. M. Benedikt, A. Fabich, S. Hancock, M. Lindroos, EURISOL DS/TASK12/TN-05-03
52. MONOLITH Collaboration, N.Y. Agafonova et al., LNGS-P26-2000, LNGS-P26-00, CERN-SPSC-2000-031, CERN-SPSC-M-657
53. INO Collaboration, M.S. Athar et al., India-based Neutrino Observatory: Project Report. Vol. I, INO-2006-01
54. R. Gandhi, P. Ghoshal, S. Goswami, P. Mehta, S. Uma Sankar, Phys. Rev. D **73**, 053 001 (2006)
55. MINOS Collaboration, P. Adamson et al., Phys. Rev. D **75**, 092 003 (2007)
56. V. Agrawal, T.K. Gaisser, P. Lipari, T. Stanev, Phys. Rev. D **53**, 1314 (1996)
57. M. Gluck, E. Reya, A. Vogt, Z. Phys. C **67**, 433 (1995)
58. GEANT – Detector Description and Simulation Tool CERN Program Library Long Writeup W5013
59. P. Picchi, F. Pietropaolo, ICGF Internal Note 344/1997, available as CERN Preprint SCAN, SCAN-9710037
60. V. Agrawal, T.K. Gaisser, P. Lipari, T. Stanev, Phys. Rev. D **53**, 1314 (1996)
61. M. Ambrosio et al., Nucl. Instrum. Methods A **456**, 67 (2000)